Nucleic Acids Research, 1995, Vol. 23, No. 24 5055–5063

A novel PRD I and TG binding activity involved in virus-induced transcription of IFN-A genes

Pierre Génin, Jose Bragança, Nicole Darracq, Janine Doly and Ahmet Civas*

Laboratoire de Régulation de l'Expression des Gènes Eucaryotes, CNRS, UPR 37, UFR Biomédicale des Saints-Pères, Université René Descartes, 45 rue des Saints-Pères, 75270 Paris Cedex 06, France

Received July 25, 1995; Revised and Accepted November 3, 1995

ABSTRACT

Comparative analysis of the inducible elements of the mouse interferon A4 and A11 gene promoters (IE-A4 and IE-A11) by transient transfection experiments, DNase I footprinting and electrophoretic mobility shift assays resulted in identification of a virus-induced binding activity suggested to be involved in NDV-induced activation of transcription of these genes. The virus-induced factor, termed VIF, is activated early by contact of virions with cells. It specifically recognizes the PRD I-like domain shared by both inducible elements, as well as the TG-like domain of IE-A4. This factor, distinct from the IRF-1, IRF-2 and the αF1 binding proteins and presenting a different affinity pattern from that of the TG protein, is proposed as a candidate for IFN-type I gene regulation.

INTRODUCTION

Transient transcriptional activation of different members of the Interferon A (IFN-A) multigene family, which belongs to the IFN type I group, is a primary cellular response to viral infection. It occurs predominantly in human leukocytes and lymphoid cells and essentially in fibroblastic cells and macrophages in the mouse (1–5). Expression of IFN-B, another type I IFN gene, is essentially restricted to fibroblastic cell lines in both species (1,4). Studies performed in stable or transiently transformed mouse L cells induced with the Newcastle disease virus (NDV) have shown that human IFN-A1 gene transcription is mediated by a 46 bp fragment, known as the virus responsive element (VRE-A1), extending from –109 to –64 nt upstream from the transcription start site (6,7). Similarly, the region denoted the inducible element and extending from –109 to –75 nt was shown to confer NDV inducibility on the murine IFN-A4 gene promoter (8,9). The inducible element IE-A4, which shares extensive homology with human VRE-A1, was shown to contain an inducible [–109 to –96] and a constitutive [–96 to –88] domain (9).

These virus responsive sequences, which regulate differential expression of the IFN-A genes in a given cell type, exhibit similarities with the minimal virus responsive part of the regulatory region of the IFN-B gene promoter (10). This region, also denoted VRE-β, is composed of different positive and negative regulatory domains (PRD and NRD). The latter, it has been suggested, maintain a state of poised repression (10–14). Virus-induced transcription and post-inductional repression were shown to be essentially mediated by the PRD I domain, described as the binding site for the nuclear factors IRF-1 (interferon regulatory factor 1) and IRF-2 (15–17) and by the PRD II domain recognized by NFκB (nuclear factor κB) and HMGI(Y) (high mobility group proteins) (18–25). These domains function as virus inducible enhancers when present in two or more copies or in combination with the other (21,24,25). The PRD III binding proteins (IRF-1 and IRF-2) and the PRD IV binding factor ATF-2/CRE-BP1 (a member of the activating transcription factor/cAMP response element binding protein family) were shown to be required for maximal levels of virus induction of the human IFN-B gene in mouse L929 and human HeLa cells (26).

The high degree of homology between the [–98 to –87] region of IFN-A genes and the PRD I domain of IFN-B has raised the possibility of a common transactivation pathway involving IRF-1 in NDV-induced expression of type I IFN (17,27,28). In fact, IRF-1 was shown to induce expression of murine IFN-A4 and IFN-A6 gene promoters in transient transfection assays without affecting expression of endogenous IFN-A genes (29).To explain this result a cooperation between IRF-1 and a factor called αF1/B was proposed. These factors, binding respectively to the PRD I-like motif and to the overlapping GTAAAGAAAGT sequence of the promoter, were suggested to be required for NDV-induced IFN-A4 gene expression in murine L929 cells (30,31).

Recent data obtained from targeted gene disruption experiments on NDV-induced transcription of type I IFN genes have somewhat modified the critical role attributed to IRF-1 in their regulation (32,33). The similarity of NDV-induced IFN-B and IFN-A transcript levels between the fibroblasts of IRF-1 gene-deficient mice and wild-type mice showed that IRF-1 is not necessary for activation of type I IFN genes. The synergistic effect of IRF-1 and other factors on the delayed response of different cell lines to cytokine or IFN-γ treatment (34–37) seemed also not to operate in virus-induced activation of transcription. In contrast, the repressor effect of IRF-2 was confirmed by up-regulation of type I IFN gene expression in NDV-induced fibroblasts where the IRF-2 gene was disrupted (32).

Another factor which has been suggested to be involved in IFN-A gene regulation is referred to as the TG protein (38,39). This factor, which remains to be characterized, was shown to specifically recognize the GAAATGGAAA sequence located in human VRE-A1 between nt –84 and –75. The TG protein and the αF1 binding factors mentioned as specifically involved in IFN-A

* To whom correspondence should be addressed

gene regulation indicate the existence of different pathways mediating virus inducibility of the IFN-A and IFN-B genes.

Within a 40 kb murine genomic fragment we have isolated three new IFN-A genes, namely IFN-A7, IFN-A8 and IFN-A11, which encode biologically active proteins (40–42). RNase protection experiments have revealed that the IFN-A11 gene was very weakly induced by NDV in L929 cells as compared with IFN-A4 and IFN-A2 (2,40). A striking homology was observed between the 5′-flanking sequences of the highly inducible IFN-A4 promoter and IFN-A11, particularly in their [–109 to –64] region containing the inducible element. In fact, these regions only differ by an A→G substitution at position –78. We have previously shown the negative effect of this mutation on NDV-induced transcription of the IFN-A11 promoter in L929 cells. We have also pointed out that the reduced level of IFN-A11 gene expression was, in part, due to the presence of negatively acting sequences located upstream of the inducible element (43).

In this report we have comparatively analysed the IFN-A4 and IFN-A11 promoters to identify the complexes specific for their inducible element, which could account for their differential response to NDV induction. We identified a virus-induced complex containing a factor which specifically recognizes the PRD I-like domain of both promoters and the TG-like domain of the IFN-A4 inducible element. This factor, suggested to be involved in IFN type I gene regulation, presents various features different from previously described PRD I binding activities.

MATERIAL AND METHODS

Plasmid constructions

The pV4 and pV11 constructs were obtained by insertion of synthetic [–112 to –64] fragments of the IFN-A4 and IFN-A11 promoters at the *Hin*dIII and *Bam*HI sites upstream of the [–39 to +51] region of the herpes simplex virus thymidine kinase promoter (pBLCAT2, modified by G. Schütz) fused to the *CAT* gene (44). Insertion of the [–112 to –82] region of the IFN-A4 promoter was as described above to obtain the pAB plasmid. For construction of the p[C4], p[C11] and p[B] plasmids synthetic oligomers corresponding respectively to the [–85 to –74] subdomains of the IFN-A4 and IFN-A11 inducible elements and to the [–98 to –87] region shared by both promoters were inserted either in single copy or in tandem in both orientations at the blunted *Sal*I site of the modified pBLCAT2 plasmid.

Transfection and CAT assays

Mouse L929 cells (ATCC CCL1) were seeded at 2×10^5 cells/35 mm dish in Dulbecco's modified Eagle's medium (Gibco, Gaithersburg, USA) supplemented with 10% horse serum. Cells were transfected with 1.25 µg total plasmid DNA by the calcium phosphate method, treated 4 h later with 12% glycerol for 1 min and induced by NDV or mock-induced as previously described (43,45,46). Measurements of CAT activity were performed on cytoplasmic extracts obtained 24 h after induction (47). Protein concentration was determined by the Coomassie G250 procedure, using bovine serum albumin as standard (48). The results are derived from CAT values obtained in at least three independent transfection experiments, each performed in triplicate.

Preparation of nuclear extracts

L929 cells (8×10^9) were grown in suspension in Dulbecco's modified Eagle's medium supplemented with 10% fetal calf serum. Virus induction was performed with NDV for 1 h as described above. For cytokine induction recombinant mouse IFN-α11 was added to the culture medium for 2 h at a concentration of 10^3 U/ml. After washing and centrifugation of the cells immediately after harvesting nuclear extracts were prepared according to Dignam *et al.* (49). For kinetics studies, performed in the absence or in the presence of cycloheximide (50 µg/ml), 5×10^8 L929 cells were induced with NDV for 1 h and cultured for varying time periods.

Gel mobility shift assays

Oligonucleotides used in EMSA are described in Figure 2. Double-stranded oligomers corresponding to different Ets binding sites were synthetized according to John *et al.* (50). Preparation of the probe was performed using single-stranded oligonucleotides 5′-labelled with [γ-^{32}P]ATP (3000 Ci/mmol; Amersham, Little Chalfont, UK) and annealed to a slight excess of the unlabelled complementary strand. Binding reactions for EMSA occurred in a final volume of 10 µl containing 10 µg nuclear extract, 2 µg poly(dG–dC)·poly(dG–dC), 0.2% Nonidet P-40, 10 mM Hepes–KOH, pH 7.9, 40 mM KCl, 0.2 mM $MgCl_2$, 1 mM EDTA, 1 mM dithiothreitol (DTT), 2% glycerol and 0.1 mM phenylmethylsulfonyl fluoride (PMSF). This mixture was incubated for 10 min at 4°C before addition of 15–20 fmol radiolabelled probe. Binding reactions were performed at room temperature for 30 min. After adding 2 µl loading dye (80% saccharose, 10 mM Hepes, pH 7.9, 0.1% bromophenol blue) the samples were loaded onto a 7% polyacrylamide gel (30:1 acrylamide:bisacrylamide) pre-run for at least 2 h in 25 mM Tris, pH 7.9, 25 mM boric acid, 0.5 mM EDTA. Electrophoresis was performed for 4–6 h at 150 V at 4°C. The gel was then dried and autoradiographed. For experiments using antibodies the nuclear extract was pre-incubated for 1 h on ice with antisera before addition of the binding reagent and the labelled probe. For competition assays a 200-fold molar excess of unlabelled competitor DNA was mixed with the probe prior to addition of the nuclear extract. In all experiments presented in this paper the same EMSA patterns were obtained when 1 µg poly(dI–dC)·poly(dI–dC) was used instead of 2 µg poly(dG–dC)·poly(dG–dC).

DNase I footprinting experiments

L929 cells were infected with NDV for 1 h (including the adsorption period) at a multiplicity of infection of 1. They were then immediately harvested for preparation of nuclear extracts, which were submitted to heparin–Sepharose CL-6B™ chromatography (Pharmacia, Uppsala, Sweden) eluted step-wise with Hepes–KOH buffer, pH 7.9, containing increasing concentrations of KCl. The fraction eluted with 0.4 M KCl was precipitated with 3.8 M ammonium sulfate at 4°C and dialysed against buffer C (49). This fraction, which contained most of the binding activity in EMSA, was used in DNase I footprinting experiments. The probes consisted of *Hin*dIII–*Bam*HI fragments isolated from pIF4J and pIF11J plasmids containing the [–119 to +19] promoter region of the IFN-A4 and IFN-A11 genes respectively. These constructs resulted from subcloning of the amplified fragments obtained by PCR using the pIF4T and pIF11T plasmids (43) as templates. DNAs were labelled at the *Hin*dIII site for the

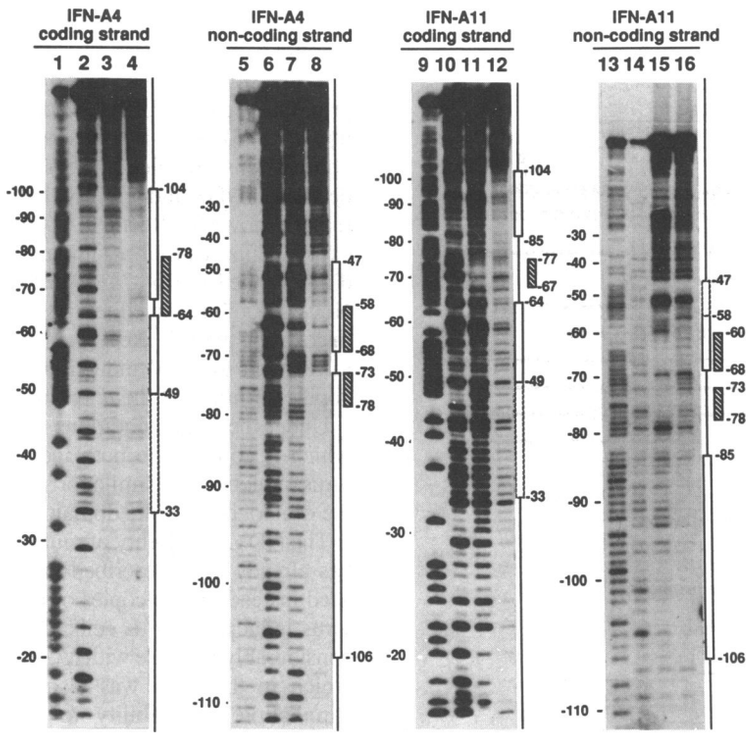

Figure 1. Effect of NDV induction on DNase I footprints of IFN-A4 and IFN-A11 promoters deleted up to position –119. Induced nuclear extracts were obtained from cells immediately harvested after being kept in contact with NDV for 1 h. Partially purified 0.4 M KCl fractions eluted from heparin–Sepharose chromatography containing the principal binding activity were used in the binding mixtures. The 3′-end-labelled DNA fragments were incubated in the absence (lanes 2, 6, 10 and 14) or in the presence of uninduced (lanes 3, 7, 11 and 15) and NDV-induced L929 nuclear extracts (lanes 4, 8, 12 and 16). They were then subjected to DNase I digestion (0.5 U for free DNA and 6 U for DNA in the presence of extracts) and analysed on a 6% sequencing gel. Maxam and Gilbert A+G (lanes 1 and 9) and C+T (lanes 5 and 13) ladders were generated and displayed for each labelled DNA. The DNase I-protected regions under uninduced and NDV-induced conditions are represented by hatched and open boxes respectively. Light stippled boxes indicate additional protected regions observed under NDV-induced conditions.

non-coding strand and at the *Bam*HI site for the coding strand with [α-^{32}P]dATP and [α-^{32}P]dCTP using DNA polymerase Klenow fragment. Probe DNA (15–20 fmol, 3 μCi/pmol) was incubated in a reaction mixture containing 0.2% Nonidet P-40, 10 mM Hepes, pH 7.9, 40 mM KCl, 0.2 mM $MgCl_2$, 1 mM EDTA, 1 mM DTT, 2% glycerol, 0.1 mM PMSF in the presence or absence of 25 μg nuclear extracts for 30 min at room temperature. Digestion by 0.5–6 U DNase I (Pharmacia) was performed as described by Galas and Schmitz (51). Digestion products were run on a 8% polyacrylamide–7 M urea sequencing gel at 60 W (1500 V, 25 mA) for 3 h.

Laser cross-linking experiments

A gel shift assay performed on a preparative scale was used in these experiments. The binding mixture containing the DNA probe in the presence of NDV-induced crude nuclear extracts was irradiated according to Hockensmith *et al.* (52) at 266 nm for 5 ns with a Nd:YAG laser (Spectra-Physics Inc., Mountain View, CA) generating an average power output of 80 mJ/pulse. The mixture was then loaded on a 7% polyacrylamide gel and after autoradiography of the wet gel the slice containing the complex was excised, equilibrated in Laemmli buffer for 30 min and submitted to SDS–PAGE (53). Image acquisition was with a PhosphorImager (Molecular Dynamics 445-SI) and the apparent molecular weight of the covalently cross-linked nucleoprotein species was calculated using ^{14}C-labelled Rainbow^{TM} protein markers (Amersham, Little Chalfont, UK) as standards.

RESULTS

NDV induction affected the DNase I footprint patterns of IFN-A4 and IFN-A11 promoters differently

The difference in the NDV-induced expression levels of two members of the IFN-A multigenic family, namely IFN-A4 and IFN-A11, was shown to be due to the –78A→G substitution in their inducible elements and to the presence of negatively acting sequences located between –470 and –200 (43). We analysed the effect of the –78A→G substitution on protein–DNA interactions occurring in the inducible element by DNase I footprint experiments using the [–119 to +19] fragment of these two genes.

The DNase I footprint patterns of both promoters did not reveal any significant difference when uninduced nuclear extracts were used. Under these conditions the protection is restricted to the [–78 to –60] region (Fig. 1, lanes 3, 7, 11 and 15). Virus induction (L929 cells kept in contact with NDV for 1 h) considerably modified these patterns. Actually, a larger protected region encompassing –106 to –70 was detected on both strands of the IFN-A4 promoter fragment (Fig. 1, lanes 4 and 8). This interaction domain corresponds to IE-A4, previously delineated

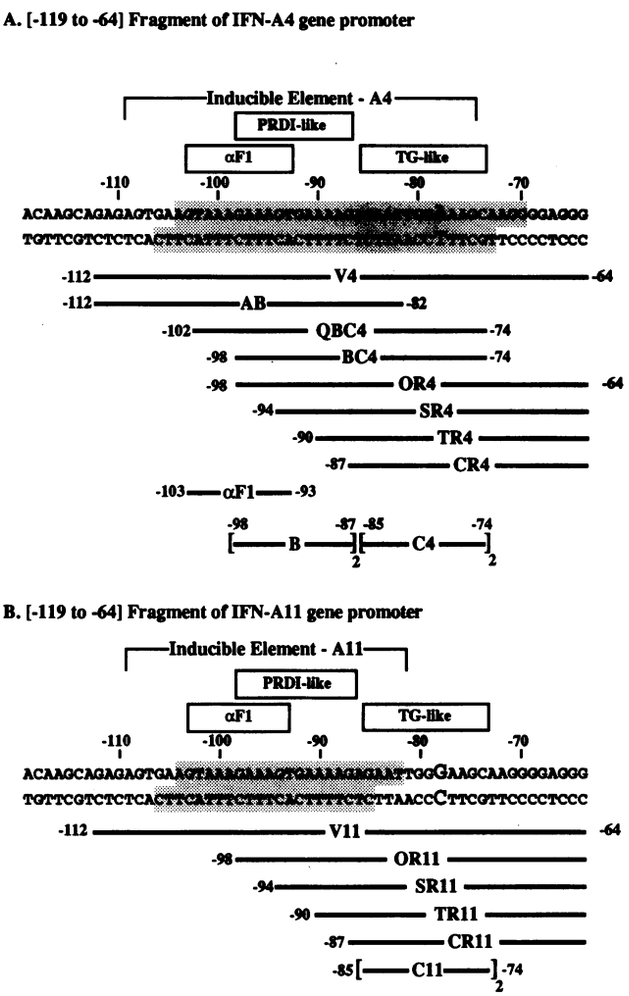

Figure 2. Sequence comparison of the [–119 to –64] fragment of the IFN-A11 (**A**) and IFN-A4 (**B**) promoters. Numbering is relative to the initiation site of transcription. The –78 nucleotide substitution is denoted by larger characters. The inducible element of the IFN-A4 gene promoter delineated by Raj *et al.* (8,9) is indicated. Localization of the binding sites for potential transactivators of the murine or human IFN-A genes αF1 (30), PRD I (15) and TG (38) are indicated above the sequences. The shaded nucleotides correspond to the NDV-induced interaction domains revealed by the DNase I footprint analysis. The double-stranded oligomers used as probes and/or competitors in EMSA are noted below the sequences.

by mutational analysis of the promoter (9). The protection pattern observed under induced conditions within the IFN-A11 promoter was limited to the [–106 to –85] region (Fig. 1, lanes 12 and 16). Binding of factors interacting with IE-A4 is obviously affected by the –78A→G mutation in NDV-induced cells.

Another interaction domain was observed between the inducible element and the TATA box on both promoters, particularly after NDV induction. The effect of this domain, spanning nt –64 to –43, on virus-induced transcription remains to be established.

Effect of the proximal part of the inducible element on virus-activated transcription

To determine the subdomain of the inducible element which affects NDV inducibility and the DNase I protection patterns of the IFN-A4 and IFN-A11 promoters, oligonucleotides corresponding to different subdomains of both inducible elements (see Fig. 2) were inserted upstream of the HSV *tk* promoter in the modified pBLCAT2 plasmid and were transiently transfected into L929 cells.

The results of these transfections clearly indicated that the proximal region of IE-A4 is actually required for virus inducibility (Fig. 3). Our conclusion is based upon the following observations: (i) deletion of the [–81 to –64] region considerably decreased NDV inducibility; (ii) the –78A→G mutation in this region, shown to affect DNA–protein interactions in footprinting experiments, caused a similar decrease in inducibility; (iii) a dimer of the [–85 to –74] region of the IFN-A4 promoter confers NDV inducibility in either the sense or antisense orientation; (iv) in contrast, the TG-like sequence of the IFN-A11 promoter failed to respond to NDV induction, even when inserted in multiple copies upstream of the *tk* promoter.

Under the same conditions dimers of the PRD I-like domain, which is common to both inducible elements, also respond to virus induction to a similar or stronger extent as that conferred by the dimerized TG-like domain of IE-A4.

The NDV nducibility of multimers of the PRD I-related motifs has already been described (23,25,39,54). $(AAGTGA)_4$, often used instead of two copies of the genuine PRD I motif, showed virus inducibility in L cells (23,24). Inducibility was shown to considerably increase with $(AAGTGA)_8$, referred to as $(PRD\ I)_4$, which in this case was also inducible by IFN-β and IFN-γ stimulation. The ability to respond to IFN treatment was attributed to the sequence similarity of this multimerized motif to the AAGTGAAACTGA part of the ISRE sequence. The authors have also found that $(AAGTGA)_4$ (or two copies of PRD I) cannot be stimulated by IFN treatment. Consistent with these results, none of the constructs pV4, pV11, pAB, $p[B]_2$, $p[C4]_2$ and $p[C11]_2$ induced with recombinant IFN-α respond to IFN stimulation.

Complexes detected by EMSA with the PRD I-like domain

To characterize specific nucleoprotein complexes containing factors potentially involved in viral induction of the IFN-A4 and A11 genes we performed EMSA using as probes different series of oligonucleotides containing subdomains of their inducible elements (Fig. 2). Nuclear extracts were prepared from L929 cells infected by NDV and harvested at different times after infection.

EMSA with oligomer $[B]_2$, corresponding to the dimer of the PRD I-like domain, revealed that NDV induction results in the appearance of a complex within 1 h of contact between cells and virus. This binding activity is progressively enhanced up to 8 h, peaking by the 6 h, but is not detected 24 h after infection. The time course of formation of the virus-induced complex, termed VIC, was unaffected by the presence of cycloheximide (Fig. 4A). This result showed that the virus-induced factor, VIF, constituting this complex pre-exists in the cells and is activated by a post-translational modification in response to viral induction.

Consistent with this observation, in uninduced cells we detected a complex corresponding to VIC only in cytoplasmic extracts and no equivalent binding activity in uninduced nuclei was detected, even after extended exposure times (Fig. 4A and B, lanes 1). The absence of a significant increase in binding activity of this cytoplasmic fraction after up to 6 h induction suggested that VIF translocates to the nucleus after induction.

Competition experiments with various oligonucleotides were performed to delineate the binding site of this factor. Figure 5

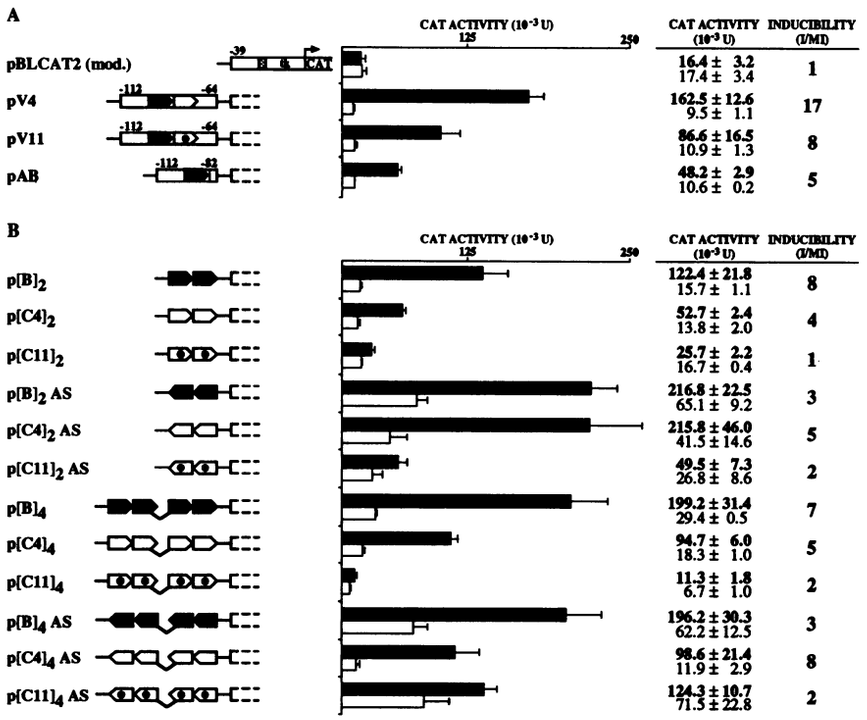

Figure 3. Effect of the [–85 to –74] proximal region of IE-A4 on virus-induced transcription. (**A**) The [–112 to –64] fragments of the IFN-A4 and IFN-A11 promoters and the [–112 to –82] fragment shared by both promoters, inserted upstream of the [–39 to +51] region of the herpes simplex virus thymidine kinase (*tk*) promoter in the modified pBLCAT2 plasmid, are represented to the left of the figure. The shaded box corresponds to the TATA box. Black and white boxes correspond respectively to the PRD I-like domain and to the TG-like domain of the IFN-A4 and IFN-A11 promoters. The –78A→G substitution in the TG-like domain of IE-A11 is indicated by a black point. (**B**) The TG-like [–85 to –74] domains of IFN-A4 and IFN-A11 and the PRD I domain [–98 to –87] common to both promoters were inserted in tandem, either in the sense or antisense orientation. The residual polylinking site resulting from the insertion of two copies of the tandem is indicated by a broken line. These constructions were transfected into L929 cells as described in Materials and Methods, induced with NDV (black bars) or mock-induced (white bars). The bar values represent the average of CAT activities expressed in bacterial CAT units, obtained in at least three independent transfection experiments. The standard deviations of the means are indicated. Inducibility values correspond to the ratio of NDV-induced (bold type) to mock-induced CAT activities.

shows their ability to inhibit formation of VIC. The specificity of VIC was shown by its competition with a 25-fold molar excess of unlabelled $[B]_2$ (Fig. 5B). Formation of VIC is also specifically inhibited by a dimer of the TG-like sequence of IE-A4, represented by $[C4]_2$, suggesting that VIF recognizes both the PRD I-like and TG-like subdomains. Consistent with this observation, the C13 oligomer (15), composed of three consecutive repeats of the motif AAGTGA, and the $(GAAATG)_4$ oligomer, described as the binding site for TG protein (38), were also efficient competitors of VIC, indicating that VIF recognizes specifically GAAAGT or GAAATG repeats with the same affinity or with an affinity slightly higher than for the GAAAGT motif (Fig. 5B). Thus it seemed to be different from TG protein, which was shown to exhibit a higher affinity for the $(GAAATG)_4$ sequence.

Multimers of the GAAATG and GAAAGT motifs also inhibit formation of other complexes shown to contain IRF-2 (see below), in contrast to $[C4]_2$, which only affects VIC. Strikingly, VIC moderately competes with the TG-like sequence of the inducible element of the IFN-A11 gene promoter, even at a 200-fold molar excess. This result indicated that binding of VIF is affected by the –78A→G substitution. Similarly, VIC is barely detected with the $[C11]_2$ probe in NDV-induced nuclear extracts (Fig. 6, lane 6). The differential competition pattern due to this mutation was also observed with V4 and V11, as well as with different oligonucleotides corresponding to 5′ deletions of their proximal part. The absence of competition with CR4 and CR11 showed that the 5′-border of the binding site of VIF extends beyond nt –87. Moderate inhibition of VIC by IE-A4-related proximal fragments (TR4, SR4 and OR4), as well as by those containing the PRD I-like motif in a single copy (AB and BC4), showed that VIF is able to bind to different enhancer domains of the inducible element, but not to the αF1 sequence. The absence of competition with this motif (Fig 5, lane 6) showed that VIF is not related to the recently described αF1 binding proteins (30).

The 'GGAA' motif found in the core sequence of binding sites for the Ets transcription factor family exists in a single copy in the [–85 to –74] region of both IE-A4 and IE-A11 and in two copies in dimers corresponding to these regions. The Ets binding motif can also be artificially created by multimerization of the motifs which compose $[B]_2$ and $(GAAATG)_4$. Inhibition of VIC formation with all these oligonucleotides could arise from a similarity between the DNA binding domain of VIF and Ets family members. However, oligonucleotides which correspond to different Ets binding sites did not react with VIC (Fig. 5, lanes 20–23). Rather, they competed with a non-specific complex of lower mobility, while the C13 oligomer, lacking this binding site, efficiently inhibited VIC formation. The Ets binding motif thus seemed not to be involved in the interaction of VIF with DNA.

Since VIF also particularly recognizes the proximal part of the inducible element of the IFN-A4 promoter and since this interaction

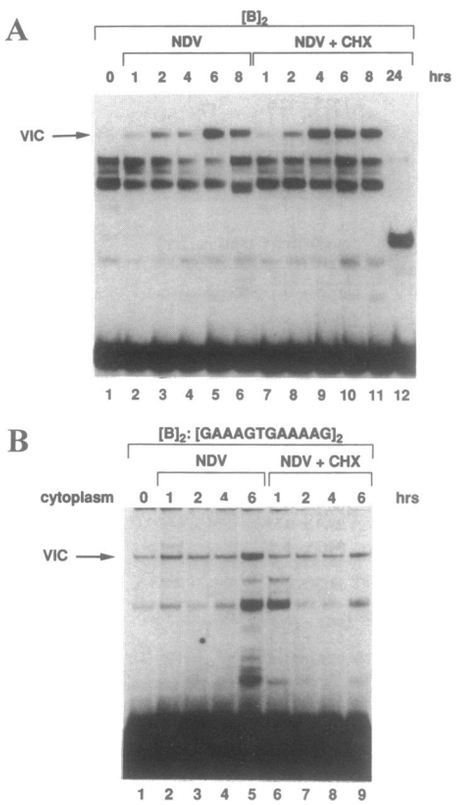

Figure 4. Time course of the virus-induced binding activity detected in EMSA with the $[B]_2$ dimer of the PRD I-like domain. Nuclear (**A**) or cytoplasmic (**B**) extracts were prepared from L929 cells uninduced (lane 1) or induced with NDV. Cells were harvested at different times post-induction as indicated above each lane, either in the absence (A, lanes 2–6; B, lanes 2–5) or presence of cycloheximide (A, lanes 7–12; B, lanes 6–9). The virus-induced complex VIC is indicated on the left.

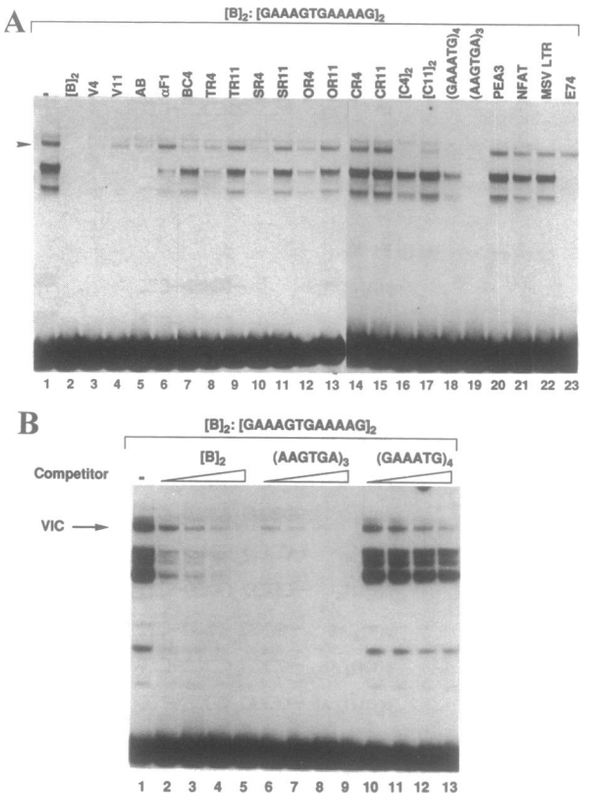

Figure 5. (**A**) Competition pattern of NDV-induced binding activity detected with the PRD I-like domain. Nuclear extracts prepared from L929 cells induced for 1 h with NDV were incubated with the $[B]_2$ probe (lane 1). Different unlabelled competitors (indicated above each lane and described in Fig. 2) were added at 200-fold molar excess (lanes 3–23), except for $[B]_2$, which was added at 100-fold molar excess (lane 2). Double-stranded oligonucleotides PEA3, NFAT, MSVLTR and E74 correspond to different binding sites for the Ets transcription factor family (50). VIC is indicated by an arrow. (**B**) Nuclear extracts prepared from L929 cells induced for 4 h with NDV were incubated with the $[B]_2$ probe (lane 1). Unlabelled competitors (indicated above) were added at 25- (lanes 2, 6 and 10), 50- (lanes 3, 7 and 11), 100- (lanes 4, 8 and 12) or 200-fold molar excess (lanes 5, 9 and 13).

is affected by the –78A→G mutation, we also used $[C4]_2$, $[C11]_2$ and SR4 as probes. Surprisingly, only one complex was observed with the dimer of the 'TG-like' region of IE-A4 (Fig. 6, lane 4). This finding is in agreement with the competition experiments, where $[C4]_2$ inhibited formation of VIC alone among the PRD I-related complexes.

The $[C4]_2$-related complex and the lowest mobility complex obtained with SR4 both showed similarities to VIC. Thus their time course of induction, their competition pattern and their gel shift mobility were indistinguishable from those observed for VIC (Figs 7 and 8). We therefore concluded that the same factor VIF is involved in formation of the $[B]_2$-, $[C4]_2$- and SR4-related complexes. These results confirmed that VIF actually recognizes the PRD I-like and the TG-like motifs of IE-A4.

The virus-induced complex did not react with the anti-IRF-1 and anti-IRF-2 antibodies

The cross-reactivity of the inducible complex VIC with the C13 oligomer, described as the high affinity binding site for IRF-1 and IRF-2, prompted us to check for the presence of IRF-1 and IRF-2 in this complex by antibody supershift analysis. Treatment of L929 cells with type I IFN was shown to induce IRF-1 binding activity (54). We therefore used as a control nuclear extracts obtained from L929 cells stimulated for 2 h with recombinant

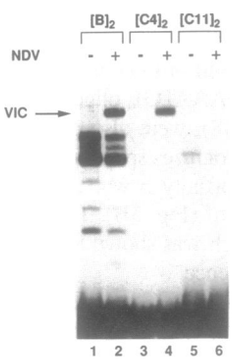

Figure 6. Comparison of the virus-induced complexes detected with the PRD I-like and TG-like domains of IE-A4. Nuclear extracts from L929 cells uninduced (–) or induced for 4 h with NDV (+) were incubated with $[B]_2$ (lanes 1 and 2), $[C4]_2$ (lanes 3 and 4) or $[C11]_2$ (lanes 5 and 6) oligonucleotides used as probes.

murine IFN-α11 protein. These experiments allowed us to identify among complexes detected with the dimer of the PRD I-like motif those containing IRF-2, which reacted equally with

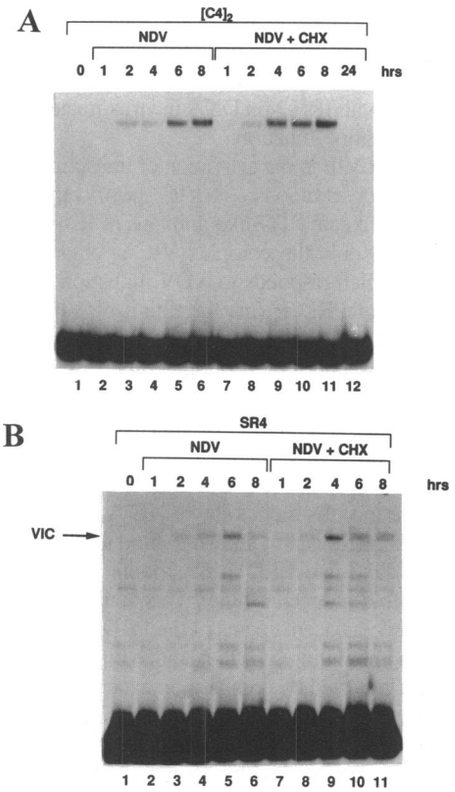

Figure 7. Time course of virus-induced complex formation detected with the TG-like domain of IE-A4 in nuclear extracts. EMSAs were performed with $[C4]_2$ (**A**), corresponding to the dimer of the [–85 to –64] region of the IFN-A4 inducible element, or with the [–94 to –64] fragment of the IFN-A4 promoter used as probes (**B**) under the same conditions as described in the legend to Figure 4A.

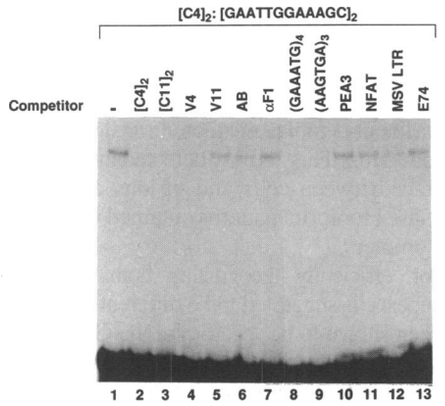

Figure 8. Competition pattern of the virus-induced complex detected with $[C4]_2$. Nuclear extracts prepared from L929 cells induced for 1 h with NDV were incubated with $[C4]_2$ probe. Different unlabelled competitors (indicated above each lane and described in Fig. 2) were added at 200-fold molar excess (lanes 2–13).

polyclonal antibodies raised against the whole murine protein or against the human IRF-2 peptide encoded by amino acids 244–258. We also visualized the complex containing IRF-1 protein specifically reacting with murine or human anti-IRF-1 antibodies (Fig. 9A). The gel shift pattern of these complexes is similar to that previously obtained by Watanabe *et al.* (54), except

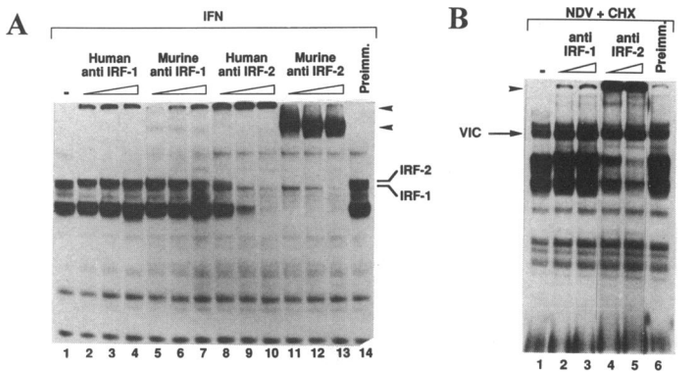

Figure 9. (**A**) Detection of the complexes containing IRF-1 and IRF-2 in IFN-α-stimulated cells. EMSAs were performed using the $[B]_2$ oligonucleotide as probe and nuclear extract prepared from L929 cells stimulated for 2 h with murine recombinant IFN-α. Extracts were pre-incubated with increasing amounts (1:40, 1:20 and 1:10 dilutions) of polyclonal antibodies raised against the [244–257] peptide of the human IRF-1 protein (lanes 2–4) or the [244–258] peptide of the human IRF-2 protein (lanes 8–10). Antibodies raised against the murine IRF-1 (lanes 5–7) or IRF-2 (lanes 11–13) proteins were also used at the same dilutions. The activity of these antibodies was controlled with recombinant huIRF-1 and huIRF-2 proteins. (**B**) Absence of reactivity of VIC with the anti-IRF-1 and anti-IRF-2 antibodies. EMSAs were performed with nuclear extracts prepared from NDV-induced L929 cells and the $[B]_2$ oligonucleotide used as probe. In this case only murine anti-IRF-1 (lanes 2 and 3) and anti-IRF-2 (lanes 4 and 5) antibodies were used at 1:40 and 1:20 dilutions. Controls were performed in the absence (lanes 1) or presence of 1 μl pre-immunization serum (A, lane 14; B, lane 6). Arrows indicate the supershifted complexes.

that we detected additional IRF-2-containing complexes of relatively high mobility. These IRF-2-related complexes are also obtained in nuclear extracts prepared from untreated cells and NDV-induced cells. In contrast, we did not detect any complex reacting with anti-IRF-1 antibodies in NDV-induced nuclear extracts (see Discussion). However, the virus-induced complex VIC reacted with neither anti-IRF-1 nor anti-IRF-2 antibodies (Fig. 9B). We therefore conclude that the factor VIF binding to PRD I-like and the TG-like domains is different from IRF-1 and IRF-2 and that it is specifically stimulated by virus induction, but not by IFN-α treatment.

DNA binding proteins of different molecular weight detected in VIC

Laser cross-linking experiments were performed in order to gain information about the molecular weight of DNA binding protein species contained in the complex VIC. As shown in Figure 10, five cross-linked products with different band intensities and corresponding to polypeptides of different molecular weights were obtained on autoradiographs of the SDS gels. The higher intensity of the 37, 44 and 57 kDa species may be due to their higher affinity for DNA and/or to the relative 'intimacy of contact' between these proteins and properly placed dT residues ideally involved in cross-linking under our UV irradiation conditions at 266 nm (52). The relation between the detected polypeptides (proteolytic cleavage, dimerization, etc.) remains to be established and further Southwestern analysis of partially purified VIF preparations obtained by PRD I or TG affinity chromatography could help to identify the specific DNA binding protein species contained in VIC. However, a heteromeric structure of VIF should not be excluded. In this case VIF would

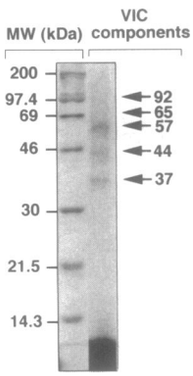

Figure 10. Determination of VIC DNA binding polypeptides by laser cross-linking experiments. EMSA was performed on a 5-fold preparative scale with the $[B]_2$ probe and nuclear extracts from L929 cells induced for 4 h with NDV. After laser irradiation of the binding mixture (see Material and Methods) VIC was excised from 7% PAGE and the slice submitted to 12.5% SDS–PAGE. The molecular weights of proteins used as standards and those of VIC components are denoted on the left and right of the autoradiograph respectively.

contain different components which, as does ISGF3, could acquire DNA binding capacity.

DISCUSSION

We identified a virus-induced binding activity detected by the GAAAGTGAAAAG and GAATTGGAAAGC sequences corresponding to the PRD I-like and TG-like motifs of the IFN-A4 promoter respectively in mouse L929 cells induced by NDV.

We showed by transient transfection experiments that both of these dimerized motifs confer virus inducibility on the minimal –39 *tk* promoter. The PRD I domain has been shown by other groups to be essential for virus inducibility of IFN-A gene promoters (30,31,39). In this way mutational analyses of IE-A4 have shown that mutations affecting residues –94 and –92 abolish activation of the IFN-A4 promoter. The PRD I domain, uninducible by itself, was suggested to act as a class A enhanson, requiring strict spacing between multimers of the same motif or two different motifs to exhibit enhancer activity (23,25). The spacing required between two motifs seemed to be preserved in our constructs carrying a dimer of the PRD I-like motif, since they clearly responded to NDV induction. The inducibility observed with the AB fragment containing the PRD I motif in a single copy can be attributed to the αF1 sequence overlapping PRD I in this construct. The integrity of the αF1 sequence, described as the binding site for a multiprotein complex denoted αF1/B, was also shown to be crucial for virus-mediated activation of IFN-A genes (30,31). It has been suggested that the complex αF1/B cooperates with IRF-1 to stabilize the weak binding of this factor to its low affinity PRD I site in IE-A4 and to induce IFN-A gene expression (31).

The stabilization of IRF-1 by another factor was also suggested by Veals *et al.* (56). The sequence similarities between ISGF3γ (the DNA recognition subunit of the IFN-α-stimulated transcriptional activator ISGF3) and IRF family members have led these authors to speculate that the functions of IRF-1, IRF-2 and other related members could depend on their ability to form complexes with as yet unidentified oligomerization partners homologous to ISGF3. Basing their argument on experiments indicating the involvement of a virus-dependent post-translational event inhibited by a serine/threonine kinase inhibitor in transcriptional activation of the IFN-B gene, they proposed that a protein component pre-existing in the cells and associating with IRF-1 on DNA in virus-treated cells could provide the transactivating function.

The involvement of VIF in the activation of transcription is based upon the following observations: (i) VIF specifically recognizes dimers of the PRD I-like and TG-like domains of IE-A4 exhibiting virus inducibility; (ii) only the complex VIC is obtained with the TG-like sequence, which responds to NDV induction at a comparable level with that of PRD I; (iii) formation of VIC is strongly inhibited by the –78A→G substitution and this inhibition can be correlated with impairment of NDV inducibility (Fig. 3, the p[C11] series of constructs); (iv) the –78A→G substitution also affects the DNase I footprint patterns of the IFN-A4 and the IFN-A11 promoter fragments in a region equivalent to their inducible element; (v) deletion of the TG-like domain recognized by VIF caused a significant decrease in virus inducibility of IE-A4. Consistent with the last finding, this factor is also shown to bind to oligonucleotides containing the TG-like and PRD I-like motifs in a single copy, although with a 2-fold reduced affinity. This could be attributed to a requirement for two adjacent copies of the PRD I or TG motifs or a combination of both binding sites to stabilize binding of VIF. This important feature was tested by competition experiments in EMSA, but also using as probes oligomers corresponding to different 5′ deletions of the proximal part of both inducible elements. Actually, among the complexes detected with oligomers of SR and TR series in the presence of substantial amounts of competitors only formation of VIC was strongly impaired with SR11 or TR11 containing the –78A→G substitution. We therefore concluded that the factor VIF binds to both the PRD I-like and TG-like motifs of IE-A4 and that the high level of inducibility of IE-A4 is due to binding of this factor on the second enhancer motif, which is defective in IE-A11.

Enhancement of the binding activity of this factor observed up to 6–8 h after viral infection in the nuclei and the absence of an equivalent binding activity in the nuclei of uninduced cells and the presence of a weak and nearly constant binding activity in the cytoplasmic fraction of uninfected and NDV-induced cells argue in favour of a latent cytoplasmic factor translocated to the nucleus upon viral induction. This activity detected in the nuclei after only 1 h of contact between cells and virions can account for the different DNase I footprint patterns obtained with the IFN-A4 and IFN-A11 promoters.

This factor, efficiently recognizing both the GAAAGT and GAAATG repeats, is suggested to be different from the TG protein which has been shown to be specific for the GAAATG motif (38). Furthermore, the absence of competition between the αF1 sequence and formation of VIC strongly suggests that VIF is not be related to the αF1 binding proteins, even though an interaction of VIF with these proteins cannot be excluded. Finally, we showed that this PRD I binding factor did not react with either anti-IRF-1 or anti-IRF-2 antibodies.

Taken together these results indicate that VIF participates in virus-activated transcription of IFN-A genes. The reactivity of this complex with the C13 oligomer, also used as a probe in separate experiments and tested to provide identical results (data not shown), suggests that VIF also participates in PRD I-mediated transcription of the IFN-B gene. This factor may play the role previously assigned to IRF-1 and may correspond or may be a part of the latent constitutive pathway activated by virus infection and postulated to mediate virus induction of type I IFN genes. The possible

heteromeric structure revealed by laser cross-linking experiments suggests that VIF could also correspond to the unidentified oligomerization partner which, as in the case of ISGF3 (56), can form multiprotein complexes with different members of the IRF family. The primary action of VIF in transcriptional activation may be further modulated by IRF family members or other PRD I binding factors.

ACKNOWLEDGEMENTS

We are grateful to Malcolm Buckle and Henri Buc for allowing us to perform the laser cross-linking experiments. We are indebted to Moshe Yaniv for his critical reading of the manuscript. We are also indebted to Nobumasa Watanabe and Tadatsugu Taniguchi for providing us with the anti-IRF-1 and anti-IRF-2 antisera and John Hiscott for the human recombinant IRF-1 and IRF-2 proteins and for the human anti-IRF-1 and anti-IRF-2 antibodies. We thank Bruno Luckow for the pBLCAT2 plasmid. Further we thank Monique Grandin for her excellent technical assistance. This work was supported by the Centre National de la Recherche Scientifique and by grants from the Institut National de la Santé et de la Recherche Médicale (CRE), the Association pour la Recherche sur le Cancer (contrat no. 1042) and the Ligue Nationale Française contre le Cancer.

REFERENCES

1 Hiscott,J., Cantell,K. and Weissmann,C. (1984) *Nucleic Acids Res.*, **12**, 3727–3746.
2 Kelley,K.A. and Pitha,P.M. (1985) *Nucleic Acids Res.*, **13**, 825–839.
3 Kelley,K.A. and Pitha,P.M. (1985) *Virology*, **147**, 382–393.
4 Raj,N.B.K., Kellum,M., Kelley,K.A., Antrobus,S. and Pitha,P.M. (1985) *J. Interferon Res.*, **5**, 493–510.
5 Shuttleworth,J., Morser,J. and Burke,D.C. (1983) *Eur. J. Biochem.*, **133**, 399–404.
6 Kuhl,D., De la Fuente,J., Chaturvedi,M., Parimoo,S., Ryals,J., Meyer,F. and Weissmann,C. (1987) *Cell*, **50**, 1057–1069.
7 Ryals,J., Dierks,P., Ragg,H. and Weissmann,C. (1985) *Cell*, **41**, 497–507.
8 Raj,N.B.K., Engelhardt,J., Au,W.-C., Levy,D.E. and Pitha,P.M. (1989) *J. Biol. Chem.*, **264**, 16658–16666.
9 Raj,N.B.K., Israeli,R., Kellum,M. and Pitha,P.M. (1989) *J. Biol. Chem.*, **264**, 11149–11157.
10 Goodbourn,S., Burstein,H. and Maniatis,T. (1986) *Cell*, **45**, 601–610.
11 Clark,A.R. and Docherty,K. (1993) *Biochem. J.*, **296**, 521–541.
12 Goodbourn,S. and Maniatis,T. (1988) *Proc. Natl. Acad. Sci. USA*, **85**, 1447–1451.
13 Maniatis,T., Whittemore,L.-A., Du,W., Fan,C.-M., Keller,A .D., Palombella,V.J. and Thanos,D.N. (1992) In McKnight,S.L. and Yamamoto,K.R. (eds), *Transcriptional Regulation*. Cold Spring Harbour Laboratory Press, New York, NY, Vol. II, pp. 1193–1220.
14 Nourbakhsh,M., Hoffmann,K. and Hauser,H. (1993) *EMBO J.*, **12**, 451–459.
15 Fujita,T., Sakakibara,J., Sudo,Y., Miyamoto,M., Kimura,Y. and Taniguchi,T. (1988) *EMBO J.*, **7**, 3397–3405.
16 Harada,H., Fujita,T., Miyamoto,M., Kimura,Y., Maruyama,M., Furia,A., Miyata,T. and Taniguchi,T. (1989) *Nature (Lond.)*, **337**, 270–27.
17 Harada,H., Willison,K., Sakakibara,J., Miyamoto,M., Fujita,T. and Taniguchi,T. (1990) *Cell*, **63**, 303–312.
18 Bose,H.R.,Jr (1992) *Biochim. Biophys. Acta*, **1114**, 1–17.
19 Lenardo,M.J., Fan,C.-M., Maniatis,T. and Baltimore,D. (1989) *Cell*, **57**, 287–294.
20 Thanos,D. and Maniatis,T. (1992) *Cell*, **71**, 777–789.
21 Visvanathan,K.V. and Goodbourn,S. (1989) *EMBO J.*, **8**, 1129–1138.
22 Du,W., Thanos,D. and Maniatis,T. (1993) *Cell*, **74**, 887–898.
23 Fan,C.-M. and Maniatis,T. (1989) *EMBO J.*, **8**, 101–110.
24 Fujita,T., Shibuya,H., Hotta,H., Yamanishi,K. and Taniguchi,T. (1987) *Cell*, **49**, 357–367.
25 Leblanc,J.-F., Cohen,L., Rodrigues,M. and Hiscott,J. (1990) *Mol. Cell. Biol.*, **10**, 3987–3993.
26 Du,W. and Maniatis,T. (1992) *Proc. Natl. Sci. USA*, **89**, 2150–2154.
27 Miyamoto,M., Fujita,T., Kimura,Y., Maruyama,M., Harada,H., Sudo,Y., Miyata,T. and Taniguchi,T. (1988) *Cell*, **54**, 903–913.
28 Reis,L.F.L., Harada,H., Wolchok,J.D., Taniguchi,T. and Vilcek,J. (1992) *EMBO J.*, **11**, 185–193.
29 Au,W.C., Raj,N.B.K., Pine,R. and Pitha,P.M. (1992) *Nucleic Acids Res.*, **20**, 2877–2884.
30 Au,W.C., Su,Y., Raj,N.K. and Pitha,P.M. (1993) *J. Biol. Chem.*, **268**, 24032–24040.
31 Raj,N.B.K., Au,W.-C. and Pitha,P.M. (1991) *J. Biol. Chem.*, **266**, 11360–11365.
32 Matsuyama,T., Kimura,T., Kitagawa,M., Pfeffer,K., Kawakami,T., Watanabe,N., Kündig,T.M., Amakawa,R., Kishihara,K., Wakeham,A., Potter,J., Furlonger,C.L., Narendran,A., Suzuki,H., Ohashi,P.S., Paige,C.J., Taniguchi,T. and Mak,T.W. (1993) *Cell*, **75**, 83–97.
33 Reis,L.F.L., Ruffner,H., Stark,G., Aguet,M. and Weissmann,C. (1994), *EMBO J.*, **13**, 4798–4806.
34 Abdollahi,A., Lord,K.E., Hoffmann-Liebermann,B. and Liebermann,D.A. (1991) *Cell Growth Differentiat.*, **2**, 401–407.
35 Briken,V., Ruffner,H., Schultz,U., Schwarz,A., Reis,L.F.L., Strehlow,I., Decker,T. and Staeheli,P. (1995) *Mol. Cell. Biol.*, **15**, 975–982.
36 Kamijo,R., Harada,H., Matsuyama,T., Bosland,M., Gerecitano,J, Shapiro,D., Le,J., Koh,S.I., Kimura,T., Green,S.J., Mak,T.W., Taniguchi,T. and Vilcek,J. (1994) *Science*, **263**, 1612–1615.
37 Stevens,A.M., Wang,Y.-F., Sieger,K.A., Lu,H.-F. and Yu-Lee,L.-Y. (1995) *Mol. Endocrinol.*, **9**, 513–525.
38 MacDonald,N.J., Kuhl,D., Maguire,D., Näf,D., Gallant,P., Goswamy,A., Hug,H., Büeler,H., Chaturvedi,M., De la Fuente,J., Ruffner,H., Meyer,F. and Weissmann,C. (1990) *Cell*, **60**, 767–779.
39 Näf,D., Hardin,S.E. and Weissmann,C. (1991) *Proc. Natl. Acad. Sci. USA*, **88**, 1369–1373.
40 Coulombel,C., Vodjdani,G. and Doly,J. (1991) *Gene*, 104, 187–195.
41 Dion,M., Vodjdani,G. and Doly,J. (1986) *Biochem. Biophys. Res. Commun.*, **138**, 826–834.
42 Navarro,S., Dion,M., Vodjdani,G., Berlot-Picard,F. and Doly,J. (1989) *J. Gen. Virol.*, **70**, 1381–1389.
43 Civas,A., Dion,M., Vodjdani,G. and Doly,J. (1991) *Nucleic Acids Res.*, **19**, 4497–4502.
44 Luckow,B. and Schütz,G. (1987) *Nucleic Acids Res.*, **15**, 5490.
45 Gorman,C. (1985) In Glover,D.M. (ed.), *DNA Cloning—A Practical Approach*. IRL Press, Oxford, UK, Vol. II., pp. 143–190.
46 Wigler,M., Pellicer,A., Silverstein,S. and Axel,R. (1978) *Cell*, **14**, 725–731.
47 Sleigh,M.J. (1986) *Anal. Biochem.*, **156**, 251–256.
48 Sedmak,J.J. and Grossberg,S.E. (1977) *Anal. Biochem.*, **79**, 544–552.
49 Dignam,J.D., Lebovitz,R.M. and Roeder,R.G. (1983) *Nucleic Acids Res.*, **11**, 1475–1489.
50 John,S., Reeves,R.B., Lin,J.-X., Child,R., Leiden,J.M., Thompson,C.B. and Leonard,W.J. (1995) *Mol. Cell. Biol.*, **15**, 1786–1796.
51 Galas,D.J. and Schmitz,A. (1978) *Nucleic Acids Res.*, **5**, 3157–3170.
52 Hockensmith,J.W., Kubasek,W.L., Vorachek,W.R., Evertsz,E.M. and von Hippel,P.H. (1991) *Methods Enzymol.*, **208**, 211–236.
53 Laemmli,U.K. (1970) *Nature*, **227**, 680.
54 Watanabe,N., Sakakibara,J., Hovanessian,A., Taniguchi,T. and Fujita,T. (1991) *Nucleic Acids Res.*, **19**, 4421–4428.
55 Pine,R., Decker,T., Kessler,D.S., Levy,D.E. and Darnell,J.E.,Jr (1990) *Mol. Cell. Biol.*, **10**, 2448–2457.
56 Veals,S.A., Schindler,C., Leonard,D., Fu,X.-Y., Aebersold,R., Darnell,J.E.,Jr and Levy,D.E. (1992), *Mol. Cell. Biol.*, **12**, 3315–3324.